Chemical Science

Accepted Manuscript

Chemical Science

rsc.li/chemical-science

Volume 9
Number 1
7 January 2018
Pages 1-268

ISSN 2041-6539

EDGE ARTICLE
Xinjing Tang et al.
Caged circular siRNAs for photomodulation of gene
expression in cells and mice

ROYAL SOCIETY
OF CHEMISTRY

This is an Accepted Manuscript, which has been through the Royal Society of Chemistry peer review process and has been accepted for publication.

Accepted Manuscripts are published online shortly after acceptance, before technical editing, formatting and proof reading. Using this free service, authors can make their results available to the community, in citable form, before we publish the edited article. We will replace this Accepted Manuscript with the edited and formatted Advance Article as soon as it is available.

You can find more information about Accepted Manuscripts in the Information for Authors.

ROYAL SOCIETY
OF CHEMISTRY

rsc.li/chemical-science

Journal Name

ARTICLE

Selectivity control in thiol-yne click reactions via visible light induced associative electron upconversion

Julia V. Burykina,‡[a] Nikita S. Shlapakov,‡[a,b] Evgeniy G. Gordeev,[a] Burkhard König*[b] and Valentine P. Ananikov*[a]

An associative electron upconversion is proposed as a key step determining the selectivity of the thiol-yne coupling. The developed synthetic approach provided an efficient tool to access a comprehensive range of products - four types of vinyl sulfides were prepared in high yields and selectivity. Practically important, here we report the transition-metal-free regioselective thiol-yne addition and formation of the demanding Markovnikov-type product by radical photoredox reaction. The photochemical process was directly monitored by mass-spectrometry in a specially designed ESI-MS device with green laser excitation in the spray chamber. The proposed reaction mechanism is supported by experiments and DFT calculations.

Introduction

Transition-metal-catalyzed atom-economic carbon-sulfur bond construction has received significant interest in the last decades.[1,2,3,4,5] Many homogeneous and heterogeneous catalytic systems were developed for the addition reaction of thiols to alkynes, but there is still demand for a selective and simple catalytic synthesis of Markovnikov and anti-Markovnikov vinyl sulfides.[6,7,8] Reported methods for selective thiol-yne reactions require expensive metal complexes or special ligands and harsh conditions. Moreover, most catalytic systems are limited in scope and metal catalyzed reactions may contaminate the products with metal traces.[9,10,11]

Visible light photoredox catalysis has evolved into an important method in organic chemistry and can provide superior reaction conditions.[12–15] A first example of a photoredox thiol-yne click reaction under metal-free conditions with good yields and selectivity for β-vinylsulfides was reported in 2016.[16] Later, Wang and co-workers reported a photoredox process driven by 1 mol% of mesityl-10-methyl-acridinium tetrafluoroborate, providing a range of mono- and bis-substituted sulfide products.[17] However, the described processes based on photoinduced free radical chain yield exclusively the linear (anti-Markovnikov) isomers.

The situation changed after Lei and co-workers[18] published a light-mediated regioselective radical synthesis of α-substituted vinyl sulfones. The possibility to apply this protocol for branched (Markovnikov type) vinylsulfides synthesis was also demonstrated. The only one example (phenylacetylene with p-tolylthiol) gives 60% ^{1}H-NMR yield of α-vinylsulfide. On the other hand, convincing and detailed mechanistic investigations shedding light on such an uncommon change of selectivity are of much interest.

Scheme 1. Controllable switching of the reaction selectivity; argon atmosphere is not important for the formation of products **5** and **6**; 1,8-diazabicyclo[5.4.0]undec-7-ene (DBU).

Our goal was to develop a universal metal-free approach to access different thiol-yne products with high selectivity. Change of the photochemical conditions allows the control of
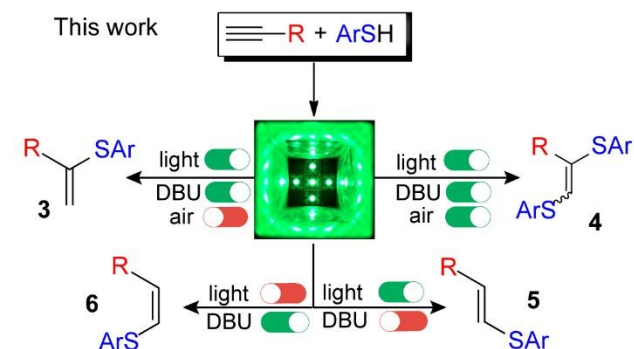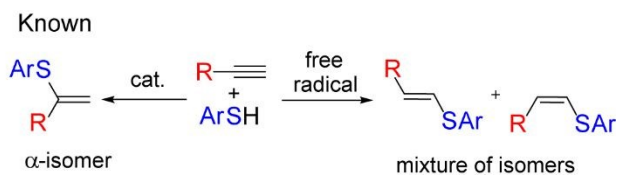
the reaction selectivity in the desired way.

a. Zelinsky Institute of Organic Chemistry, Russian Academy of Sciences, Leninsky Prospect 47, Moscow, 119991, Russia. E-mail: val@ioc.ac.ru
b. Institut für Organische Chemie, Universität Regensburg, Universitätstraße 31, 93053 Regensburg, Germany. E-mail: Burkhard.Koenig@chemie.uni-regensburg.de
† Electronic supplementary information (ESI) available: Additional experimental data, copies of NMR spectra, DFT and ESI-MS data. See DOI: 10.1039/x0xx00000x
‡ These authors contributed equally

ARTICLE

The concept behind the control of thiol addition reaction selectivity in the absence of metals relies on an associative electron upconversion consisting in highly reducing radical-anion formation via orbital crossing. The electron upconversion[21] and orbital crossing[22,23] concepts have elaborated by Alabugin and coworkers but yet has not been applied to alkyne functionalization to the best of our knowledge (Scheme 1).

In experimental and theoretical studies, we evaluated all plausible vinylsulfides/disulfides pathways of a photoredox thiol/yne reaction and determined the dependence of the selective product formation on the reaction conditions. We report a photoredox system for the synthesis of four products (α-isomer (**3**), β(E)-isomer (**5**), β(Z)-isomer (**6**) and disulfide (**4**)) under simple conditions with high selectivity (Scheme 1).
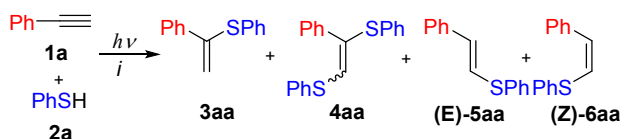
Results and discussion

The reaction of thiophenol **1a** with phenylacetylene **2a** mediated by Eosin Y under light from green light-emitting diodes (LEDs) was chosen as a model thiol-alkyne coupling (Scheme 2), but the reaction turned out to be not selective leading to the formation of a broad range of products.

Examination of typical bases revealed their crucial effect for the thiol-yne coupling. The previously reported photoredox system[16] with pyridine as base gave the anti-Markovnikov radical product **5aa** in 90% yield (Table 1, entry 1). The use of NaHCO₃ or KOAc as bases decreased yield and selectivity (entries 2-3). However, the addition of a stronger base gave an acceptable yield for product **3aa** (entry 4) what is consistent with Lei's work.[18] Additional screening revealed that moderately strong bases are necessary for obtaining the Markovnikov product **3aa** (entries 4-7). The best result gave a catalytic system of Eosin Y/1,8-diazabicyclo[5.4.0]undec-7-ene (DBU) under green LED irradiation affording the α-isomer in 85% yield (entry 7).

Further experiments revealed that air and argon have a significant influence on the selectivity of this transformation. Conducting the reaction under air and DBU gave a good yield of disulfide **4aa** (entry 8). Increasing the temperature and conducting the reaction under air without Eosin Y and light gave product **6aa** (entry 9). Formation of Z-anti-Markovnikov products under the basic conditions is discussed in Oshima's work on nucleophilic addition of thiols to alkynes.[24] Thus, a selective synthesis of **3aa/4aa/5aa/6aa** is possible by changes of the base and the presence or absence of air and light.

The concentration of reaction reagents has a significant influence on the reaction selectivity. Increasing the reagents concentration (entry 10) leads to the formation of **5aa** and **6aa** as main products and trace amounts of **3aa**. Under standard reaction conditions (entry 7) the thiol dissociates heterolytically almost completely, which prevents it from participating in the radical process leading to product **5aa**.

Table 1. Optimization of the reaction conditions and evaluation of key parameters for the reaction selectivity.[a]

Entry	Base	3aa, %	4aa, %	5aa, %	6aa, %
1	Py	0	0	**90**	10
2	NaHCO₃	29	2	62	7
3	KOAc	44	4	47	5
4	K₂CO₃	**70**	13	7	10
5	KF	**81**	7	10	2
6[b]	ᵗBuOK	33	5	0	62
7	DBU	**85**	7	3	0
8[c]	DBU	10	**77**	0	0
9[c,d,e]	DBU	0	0	7	**93**
10[f]	DBU	5	0	37	58
11[e]	DBU	0	0	0	**22**
12[e,c]	DBU	0	0	0	**23**
13[g]	DBU	0	92	0	0
14[h]	DBU	1	0	1	12

[a] Unless otherwise noted, the reactions were carried out using **1a** 0.15 mmol, **2a** 0.3 mmol, DMF 3 ml, base 0.33 mmol, Eosin Y (3 mol%), 40 °C, green LEDs (1.25 W), 24 h, argon. [b] Reaction mixture was deeply colored. [c] Under air. [d] t° = 80 °C, reaction time 72 h. [e] Reaction without Eosin Y and green light. [f] 0.125 ml of DMF. [g] Addition of TEMPO. [h] Addition of γ-terpinene. Several reaction mixtures NMR spectra are placed in SI (Figures SI 1-4).

The control reactions without Eosin Y and light irradiation, with DBU under argon (entry 11) or air (entry 12) gave the products of nucleophilic addition reactions. In case of ᵗBuOK addition the reaction mixture turns black under irradiation, and an ionic mechanism leading to by-product **6aa** prevails (entry 6).

To verify the radical pathway of the reaction we performed the transformation in the presence of radical traps: 2,2,6,6-tetramethyl-1-piperidinyloxyl (TEMPO) (entry 13) and γ-terpinene (entry 14). Presence of γ-terpinene completely suppresses any radical processes, but the background Michael-type reactivity remains. TEMPO turned out to be an ineffective radical trap in our system. It acts as one electron oxidant and can substitute air oxygen, as reflected by excellent yield of product **4aa** under these conditions.

Optimization of other reaction parameters such as reagent ratio, solvent and photoredox system are summarized in Table S1 (ESI).

Next, we studied the application of this switchable photoredox system to the synthesis of specific thiol-yne products of various alkynes. The experiments confirmed the high selectivity and efficiency of the synthetic approach for the preparation of α-isomer (**3**), β(E)-isomer (**5**), β(Z)-isomer (**6**) and bis-sulfide (**4**). In all cases, complete conversion of alkyne was achieved, and the corresponding product was obtained in good to very good yields (Scheme 3).

Scheme 2. The model thiol-yne click reaction between **1a** and **2a**.
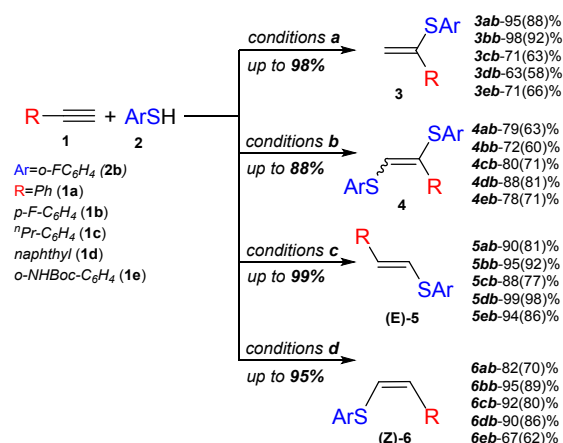
Scheme 3. Conditions **a**: (**1**) 0.15 mmol, (**2b**) 0.3 mmol, DMF 3ml, DBU 0.33 mmol, Eosin Y (3 mol%), 40 °C, green LEDs (1.25 W), 24 h, argon bubbling; **Conditions b**: under the same conditions as for [a], but (**2b**) 0.45 mmol and without argon bubbling; **Conditions c**: (**1**) 1 mmol, (**2b**) 1.1 mmol, DMF 0.5 ml, Py 0.3 mmol, Eosin Y (1 mol%), 40 °C, green LEDs (1.25 W), 6h, under air; **Conditions d**: (**1**) 1 mmol, (**2b**) 1.5 mmol, DMF 0.5 ml, ᵗBuOK 0.5 mmol, 70 °C, 24 h, under air. Yields by 1H NMR and isolated yields are shown in parentheses.

The substrate scope for the most challenging selective synthesis of the Markovnikov product (**3**) involving different types of alkynes and thiols was then investigated employing the optimized reaction conditions (Scheme 4). Due to the importance of fluorine containing compounds,[25,26,27] o-F-substituted thiol was chosen as model thiol for alkyne scope investigation. A number of aromatic thiols, bearing various functional groups at the *ortho-, meta-* and *para-* position reacted smoothly with phenylacetylene to afford the α-isomers (**3**) in 95-74% yields. Even in the case of non-polar electron-donating thiols **2a**, **2c** and **2e**, the corresponding products **3aa, 3ac** and **3ae** could be isolated in 70-78% yields.

Similarly, to phenylacetylene, terminal aromatic alkynes were selectively transformed into the expected adducts **3** in moderate to high yields. In case of electron-withdrawing alkynes **1f** and **1k** we use a more powerful 30W green LED to speed up the synthesis of the Markovnikov product and outrun the competitive non photocatalytic process of β(Z)-isomer **6** product formation. In the case of electron-donating alkynes **1g**-**1j**, the α-isomer was produced in moderate to good yields accompanied by-products **4** and **7**.

As a representative example of such side process, we investigated the reaction between **1h** and **2b** and successfully isolated and characterized compound **7hb**, the product of attack of radical **R1** at the double bond of vinylsulfide **3hb.** The electrophilic vinyl radicals get attacked by nucleophiles (**3hb** or SAr⁻), which explains why nucleophilic vinylsulfide **3hb** react in the observed manner (Scheme 5).

To determine the limitations of our method we have conducted experiments with aliphatic (**1r**) and internal (**1s**) alkynes (Scheme 6). Both alkynes react slowly under the developed conditions and full conversion was not reached after 2 days. The reaction of alkyne **1r** with such an electron-deficient thiol as **2j** gives only the oxidative product **4rj** in the absence of air. This may be explained by the formation of a highly reductive intermediate not stabilized by aromatic ring resulting in its oxidation by the solvent. On the other hand,

alkyne **1s** reacts with retention of the selectivity described above, and product **3sa** and by-product **4sa** have been isolated with overall yield of 81%. However, replacing of DBU by a weak base pyridine leads to formation of compounds **5sa** and **6sa** as expected for a free radical chain reaction.
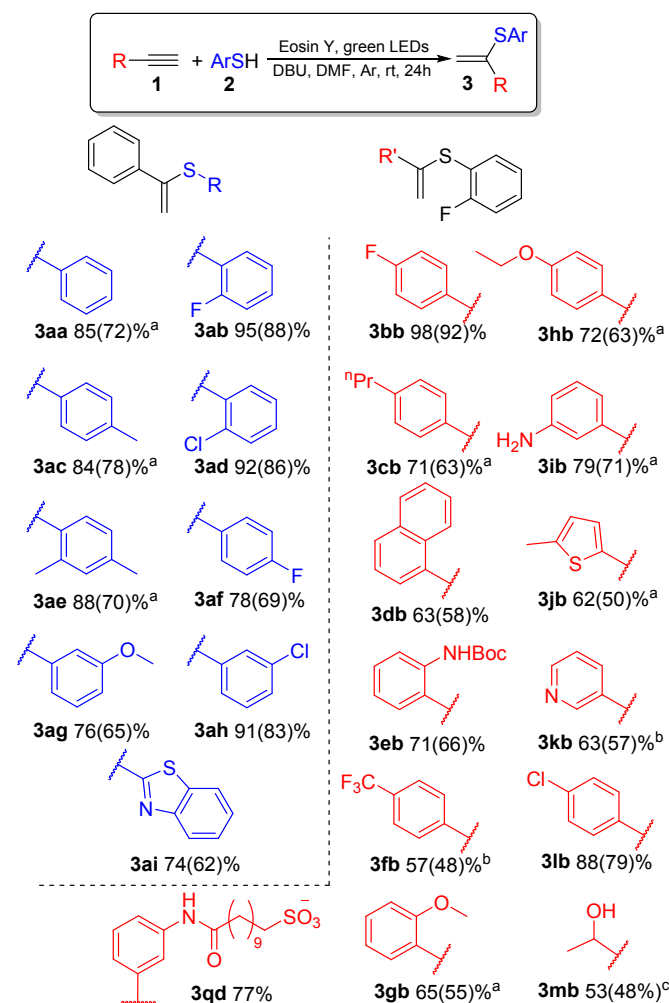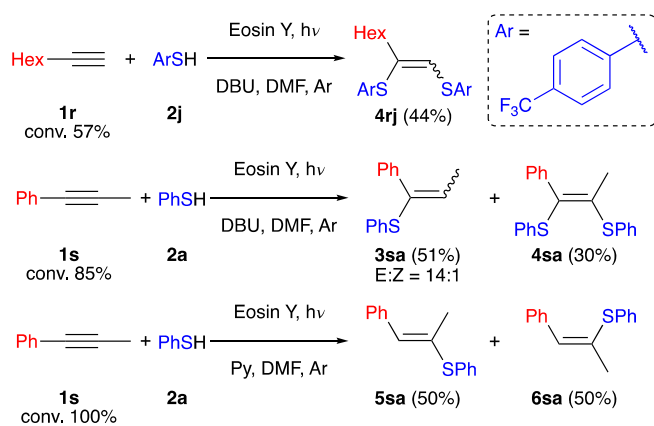

Scheme 4. Conditions: (**1**) 0.15 mmol, (**2**) 0.3 mmol, DMF 3ml, DBU 0.33 mmol, Eosin Y (3 mol%), 40 °C, green LEDs (1.25 W), 24 h, argon bubbling. Yields demined by ¹H NMR and isolated yields shown in parentheses. [a] 48h, [b] 2h, 30W green LEDs, [c] 24h, 30W.
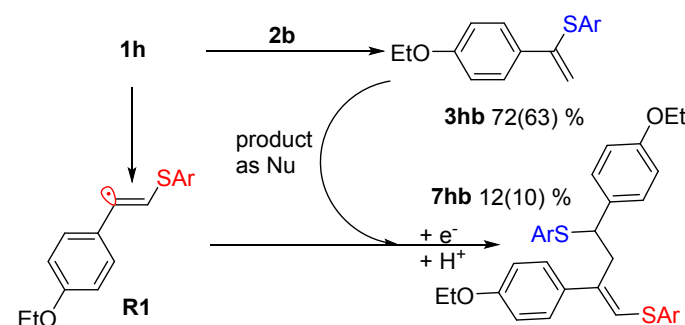

Scheme 5. Interaction between vinyl radical **R1** and vinylsulfide **3hb** under the standard reaction conditions for **7hb** formation. Yields demined by ¹H NMR and isolated yields shown in parentheses.

ARTICLE

Scheme 6. Limitations of the protocol for aliphatic (reaction conditions: **1x** 0.15 mmol, **2j** 0.3 mmol, DMF 2 ml, DBU 0.33 mmol, Eosin Y (3 mol%), 40 °C, green LEDs (1.25 W), 24h, argon flushed) and internal (reaction conditions: **1y** 0.15 mmol, **2a** 0.3 mmol, DMF 2 ml, DBU 0.33 mmol, Eosin Y (3 mol%), 40 °C, green LEDs (1.25 W), 24h, argon flushed) alkynes. The yields were determined by GC-FID.

In case of **1n** which contains an *o*-Br substituent the formation of an unexpected product **8na** was observed in 62% yield (Scheme 7). Presumably, the nucleophilic attack of the thiolate anion to the electrophilic vinyl radical **R1** via orbital crossing leads to the formation of high-reducing anion-radical **R2**. A subsequent intramolecular ET process from the π^*-orbital to the σ^*(C-Br)-orbital with consequent bromine atom extrusion gave benzothiophene derivative **8na** under loss of the Ar-radical (blue, Scheme 7), which gets trapped by a thiolate anion and oxidized.
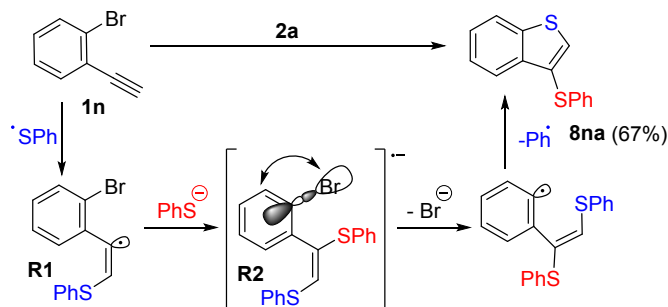
Scheme 7. Observation of IntraET between π^*-orbital of **R2** and the σ^*(C-Br)-orbital with consequent bromine atom extrusion leading to benzophenone **8nb**; reaction conditions: **1** 0.15 mmol, **2** 0.45 mmol, DMF 3ml, K$_2$CO$_3$ 0.5 mmol, Eosin Y (3 mol%), 40 °C, green LEDs (1.25 W), 24h, argon flushed. The yields were determined by ^{1}H NMR.

The similar idea to control the reactivity of substrates by intramolecular electron transfer in π-conjugated arene systems was demonstrated by Studer[28] and is applicable to other reactions with arenes.[29] Knowles[30] described the intramolecular electron transfer from a hydroxy-group to a *p*-methoxyphenyl group using photoredox catalysis supporting our hypothesis.

Further investigation of the described process led to the assumption that Intra ET is only possible when the Br-containing benzene ring (purple, Scheme 8) is in π-conjugation with the alkyne fragment (blue, Scheme 8). In the case of electron transfer via the conjugated π-system onto the σ^*(C-Br)-orbital, the C-Br bond gets activated and a radical cyclization by-product **4ob'** forms along with the main

products **3ob** and **4ob**. However, the Intra ET process depends on the spatial continuity of the upconverted anion-radical π-system. Factors that interfere with the π-conjugation between the alkyne fragment and the Br-atom containing aromatic ring (e.g. steric repulsion of peri-substituents in the biphenyl systems) may prevent the Intra ET process and lead to superiority of Intermolecular ET processes, as indicated by the predominant formation of product **4pb**.

DFT calculations of C-Br bond dissociation energy for substrates **1n**, **1o**, **1p** do not explain the low activity of **1p**. However, DFT molecular dynamics modeling has shown a significant drop of the dissociation rate of the **R2** radical anion for **1p**, because this method takes into consideration all conformations, but not the most stable one with the best conjugation (see Supporting Information and computational details).

All the findings described above highlight the key role of the upconverted **R2** radical-anion formation in the studied system.
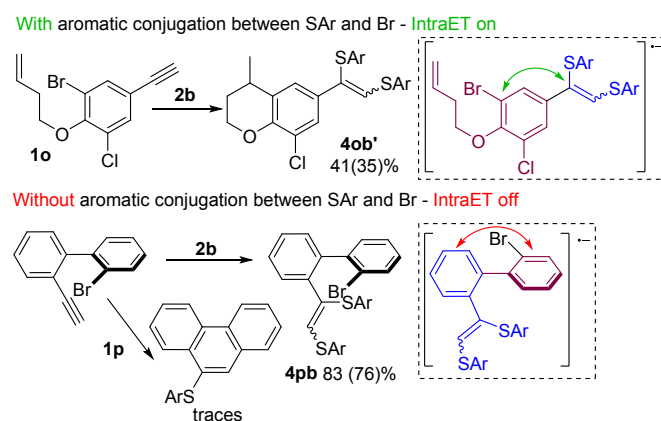
Scheme 8. Structural limitations of the IntraET process in the systems containing Br and a triple bond; reaction conditions: **1** 0.15 mmol, **2** 0.3 mmol, DMF 3ml, K$_2$CO$_3$ 0.29 mmol, Eosin Y (3 mol%), 40 °C, green LEDs (30 W), 24h, argon flushed. The yields were determined by ^{1}H NMR.

To reveal the nature of the observed transformations we carried out the reaction inside an electrospray ionization chamber of a mass spectrometer at neat state from the flask.[31,32] Monitoring of photoredox-catalyzed reactions by coupling of spray-based ionization mass spectrometers with online laser irradiation has been established as a reliable method.[33,34,35] For the thiol-yne click reaction, we coupled a green laser source with electrospray ionization mass spectrometry (ESI-MS). The device used, consisted of a green laser connected to ESI chamber as shown in Figure 1. The irradiation was directed to the tip of the nebulizer where small charged microdroplets of the reaction mixture are formed due to an applied potential between the electrode near sprayer (nebulizer is grounded) and the shield (Figure 1A).[36]

For this experiment, we have synthesized alkyne **1q** with an easily ionized sulfonate group and carried out the thyol-yne reaction between alkyne **1q** and 2-chlorothiophenol **2d** under standard reaction conditions (Scheme 4). In the negative ion mode in the absence of green light irradiation, the signals

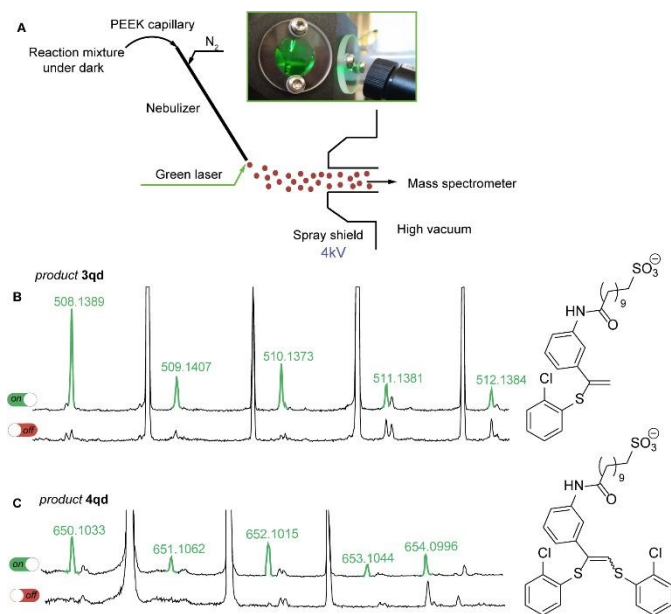corresponding to alkyne **1q**, thiol **2d**, and Eosin Y species were dominant in the ESI mass spectra.

Figure 1. a) Scheme of coupled device for online ESI-(-)MS experiment; laser power is about 80 mW. A reaction mixture was introduced into PEEK capillary after that photoexcited by the laser pointer inside spray chamber and passed into mass spectrometr; b) the real-time spectra belong to **3qd** product for light/dark experiments in negative ion mode; c) the real-time spectra belong to **4qd** for light/dark experiments in negative ion mode. Light experiment is shown in green, and dark experiment is shown in black.

Under the green light irradiation of the nebulizing tip, the molecular ions corresponding to products **3qd** (measured *m/z* 508.1389; calcd *m/z* 508.1389 for $[C_{25}H_{31}NO_4S_2Cl]^-$) and **4qd** (measured *m/z* 650.1033; calcd *m/z* 650.1032 for $[C_{31}H_{35}NO_4S_3Cl_2]^-$) began to appear a couple of milliseconds after the start of the irradiation. However, when the LED light was switched off the signals of **3qd** and **4qd** dropped to zero in their abundances (Figure 1C). Simultaneous appearance or disappearance of this peaks proved the key role of the light for the formation of a highly reactive intermediate (conceivably **R2**), which is able to transform either to the product **3** or **4**.

Furthermore, a detailed investigation of the reaction pathway by continuous online ESI-(–)MS monitoring was conducted with the irradiation of the Schlenk tube reaction vessel. This experiment allows real-time tracking of starting material, photocatalyst degradation and product formation (see Supporting Information for details).

The overall reaction mechanism is proposed on the basis of the collected experimental data and previous findings. The catalytic cycle starts from Eosin Y affording the thiyl radical upon light irradiation. Next, ArS• adds to the alkyne **1** to produce **R1,** which is able to abstract a hydrogen atom yielding side product **5,** which can be suppressed under optimized conditions. Nucleophilic addition of ArS⁻ to **R1** via orbital crossing results in the formation of **R2**. The radical-anion **R2** could be protonated, what leads to the formation of stabilized benzyl-type radical **R3**.

Subsequent elimination of a thiyl radical yields product **3**, while the ArS• radical triggers the next ion-radical cycle. It should be noted that upconverted highly reducing intermediate **R2** is extremely sensitive to oxidizing agents (oxygen impurities, excited forms of the photocatalyst or even solvent in some cases), and therefore easily diverts towards the oxidative bis-addition product **4** during the single electron transfer stage. This Inter ET process strongly depends on structure of the intermediate **R2**. The HOMO energy DFT-calculations for different **R2** demonstrates, that an aromatic substituent stabilizes the intermediate significantly better than an aliphatic one. For R = Ph, the HOMO energy is -3.40 eV, while for R = n-Hex, the HOMO energy is -3.00 eV, that is, in the case of an alkyl substituent, intermediate **R2** has significantly more pronounced electron-donating properties and can more easily lose activity due to oxidation (see Supporting Information). It explains the fact of lower yields in case **3mb** and exclusively **4rj** formation in case of aliphatic alkyne **1j**.

To support our hypothesis for the mechanism, we have measured the quantum yield at 528 nm (23%) and the quantum efficiency (29%). A high value of the quenching factor (0.8) indicates an efficient PET from the excited state of the photocatalyst to the ArS⁻ anion (E(ArS•/ArS⁻) = 0.1-0.4 V, E(Eosin*/Eosin⁻) = 0.8 V)[37], but other deactivating pathways of the photocatalyst affecting the quenching factor were not considered. The back electron transfer from the reduced form of the photocatalyst to the ArS-radical is also thermodynamically feasible (E(Eosin/Eosin⁻) = - 1.1 V).
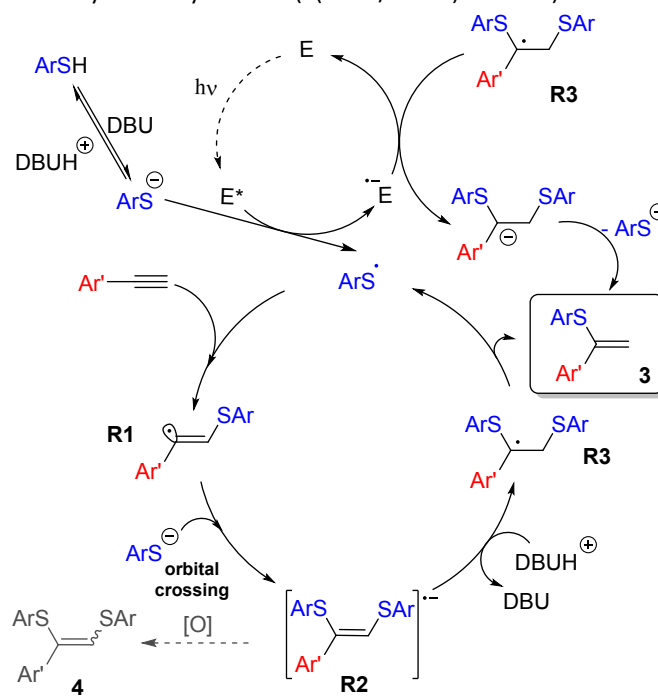

Scheme 9. Plausible catalytic cycle of the photoredox thiol-yne click reaction.

Thus, we conclude, that a short radical chain could be considered as a possible scenario for the reaction along with

moderately efficient chain termination caused by reduction of the benzylic radical intermediate **R3** (E(R3•/ R3⁻) should be less reductive then E(benzyl•/benzyl⁻) = - 1.4V because of the SAr group stabilization effect).

A

R2 (0.0; 0.0)

TS2 −10.1 / 5.1

TS1 0.2 / 14.8

R3 −15.8 / −14.4

TS3 37.2 / 36.1

E-R3 −4.1 / −5.3

3 4.8 / −9.4

E-5aa 5.3 / −9.2

B

ΔG, kcal/mol

Figure 2. A) Mechanism of product **3** formation from intermediate **R2**, which is taken as a reference point, with total energy values (ΔE, kcal/mol) denoted by green color, free Gibbs energies (ΔG, kcal/mol) denoted by red color. **B)** Representation of the free energy profile for two possible reaction paths of the product **3** formation (see conventional representation of the energy profiles and optimized molecular structures in Supporting Information); UBMK/6-311+G(d,p) D3BJ & SMD(DMF).
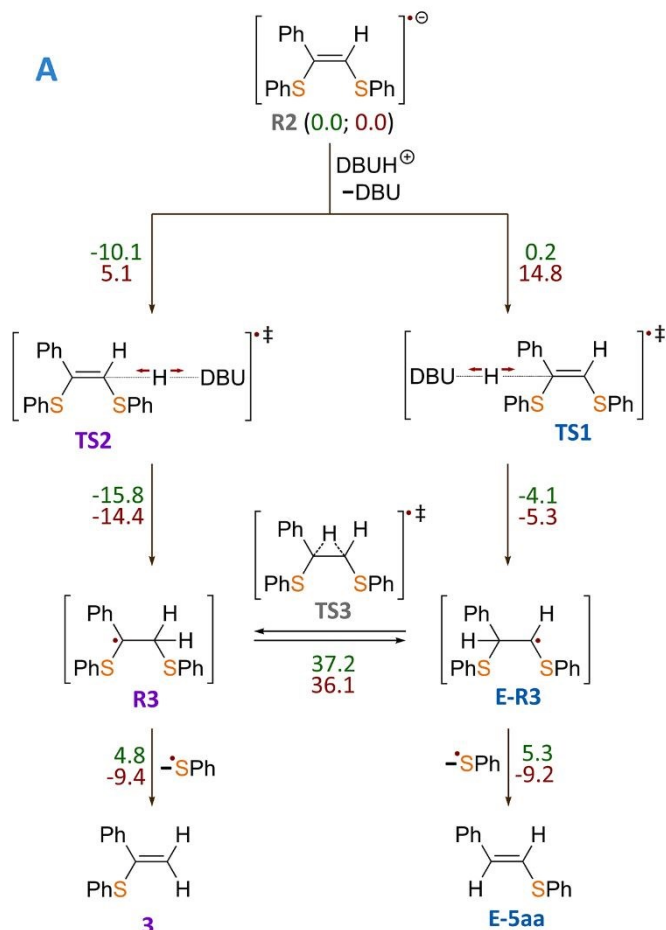
To gain insight into the radical formation and understand the reaction regioselectivity, we carried out DFT calculations of the product **3** formation from the intermediate **R2**. The transformation of intermediate **R2** to product **3** begins with protonation of one of the **R2** double bond carbons by a DBUH⁺ cation (Figure 2A). The protonation can occur either at the secondary carbon atom and proceeds via **TS2** transition state, or at the tertiary carbon atom and proceeds via **TS1** transition state. Spin density corresponding to the unpaired electron of the **R2** radical anion is predominantly localized on the C=C carbon atoms (see Figure 3A).

However, potential barriers of **R2** protonation for the two reaction channels differ significantly: the protonation leading to the anti-Markovnikov product requires much higher activation energy ($\Delta G^{\ddagger}$ = 14.8 kcal/mol) compared with the protonation leading to the Markovnikov-type product ($\Delta G^{\ddagger}$ = 5.1 kcal/mol) (Figure 2A, B). The lower activation energy for **TS2** transition state correlates with the charge distribution in the intermediate **R2**: the secondary carbon atom is negatively charged (-0.276), which ensures its increased nucleophilicity, while the tertiary carbon atom carries significant positive charge (see Figure 3B).
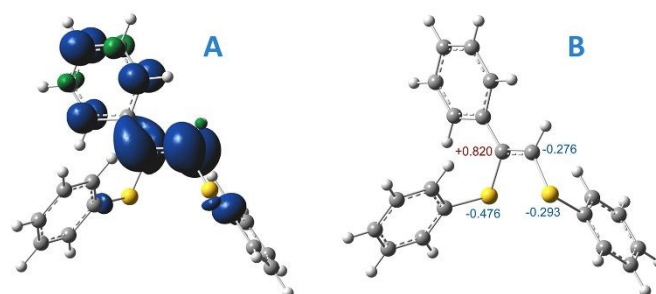

Figure 3. (A) – spin density distribution for intermediate R2; **(B)** – Mulliken atomic charges for some atoms of intermediate R2, UBMK/6-311+G(d,p) D3BJ & SMD(DMF).

Formation of product **3** is therefore promoted by kinetic and thermodynamic effects of the protonation stage: Intermediate **R3** is significantly stabilized as compared with intermediate **E-R3**. Transition between the intermediates **R3** and **E-R3** is unlikely, since the **TS3** transition state is characterized by high energy, and if the protonation proceeds via the **R2 → R3 → 3** pathway, the transition to the **R → E-R3 → E-5aa** pathway is unlikely. In the last step, regeneration of the ArS• radical occurs with the formation of the final product **3**. Within the reaction mechanism, the regeneration of Eosin Y is mediated by **R3.** Similar results were obtained for alkyl-substituted intermediate **R2** (see

Chemical Science

ARTICLE

Supporting Information). Thus, the performed calculations correlate well with our experimental findings.

Conclusions

We have developed the selective synthesis of Markovnikov-type thiol-yne products using a photoredox catalyzed reaction. The developed procedure affords Markovnikov-type vinylsulfides in up to 92% yield under mild reaction conditions. The key advantage of the developed system are simple and straightforward reaction conditions for a selective synthesis of the desired products.

Using standard ESI-MS spray-based ionization mass spectrometers with online laser irradiation, a direct monitoring of the reaction was possible. Computational study at a UBMK/6-311+G(d,p) D3BJ & SMD(DMF) level of theory revealed a lower activation energy for the Markovnikov-type product formation at the presented conditions.

Associative electron upconversion process in the photoinduced reaction of thiols and alkynes is essential for the observed selectivities. The concept may find applications in the design of other transformations of alkynes with good leaving groups based on an intramolecular electron transfer (Intra ET) process.

Experimental

General procedures

The reagents were obtained from commercial sources and used as supplied (verified by NMR prior to use). The solvents were purified according to published methods. The solvents for NMR spectroscopy were obtained from Deutero GmbH. Acetonitrile (HPLC-grade) for ESI-MS was obtained from Merck and used as supplied. Unless otherwise noted, the reactions were carried out in PTFE screw-capped tubes equipped with magnetic stirring bars. Magnetic stirring bars were cleaned with a boiling solution of alkali followed by a boiling solution of *aqua regia* and further rinsing with distilled water to ensure the removal of all absorbed metal traces. Column chromatography was performed using Merck 60 μm silica.

All NMR measurements were performed with Bruker DRX 500, Bruker Avance III 400 and Bruker Fourier 300 spectrometers operating at 500.1, 400.1 and 300.1 MHz for ^{1}H, 125, 100 and 75 MHz for ^{13}C , 470.5, 376.4 and 282.3 for ^{19}F nuclei. ^{1}H, ^{13}C{^{1}H} chemical shifts are given in ppm relative to the residual peak of the solvent DMSO-d_6 (δ 2.5 ppm) for the proton spectra and relative to solvent peak (δ 39.5 ppm) for the carbon spectra. All ^{19}F NMR chemical shifts were referenced to internal CF_3C$_6$F$_5$ (δ -55.85 ppm). The spectra were processed with Bruker TopSpin 3.2 software package.

High-resolution mass spectra were obtained on Bruker maXis Q-TOF instrument (Bruker Daltonik GmbH, Germany) equipped with an electrospray ionization (ESI) ion source. The experiments were performed in positive (+) MS ion mode (HV Capillary: -4500 V; HV End Plate Offset: -500 V) or negative (-)

MS ion mode (HV Capillary: +4000 V; HV End Plate Offset: +500 V); with a scan range of m/z 50–1500. External calibration of the mass spectrometer was performed using a low-concentration tuning mix solution (Agilent Technologies). Direct syringe injection was applied for the analyzed solutions in MeCN (flow rate: 3 μL/min^{-1}) for analytical characterization, and pressurized sample infusion was applied for reaction monitoring studies in DMF (additional experimental details provided below). Nitrogen was applied as nebulizer gas (1 bar) and dry gas (4.0 L/min, 200 °C). The spectra were processed using Bruker Data Analysis 4.0 software.

The GC-MS experiments were carried out with an Agilent 7890A GC system, equipped with an Agilent 5975C mass-selective detector (electron impact, 70 eV) and a HP-5MS column (30 m/0.25 mm/ 0.25 μm film) using helium as carrier gas at a flow of 1.0 mL min^{-1}.

The GC-FID measurements were performed with an SCION 436-GC gas chromatograph with aflame ionization detector and an HP-5MS (Agilent Technologies) column (30 m × 0.25mm × 0.25 μm film) using helium as carrier gas at a constant linear velocity of 30cm×s^{-1}. The following temperature program was used in all GC-MS measurements: initial temperature: 60 °C, hold for 2 min, then 20 °C×min^{-1} to 300 °C and hold for 6 min.

Computational Details

1. Calculations of potential energy profiles and MO analysis. All molecules were optimized by unrestricted BMK DFT method[38] in combination with 6-311+G(d,p) basis set.[39,40,41]. For more accurate description of the dispersion interaction the Grimme's D3 empirical corrections were used.[42,43] The effects of DMF media were accounted for by SMD solvation model.[44] For all structures the vibrational spectra and thermodynamic parameters were calculated at standard conditions (T = 298.15 K, p = 1 atm). All calculations were performed by Gaussian 16 software package.[45]

2. Molecular dynamics modeling.

ADMP molecular dynamics[46,47,48] modeling was performed using unrestricted BMK functional with def2SVP basis set[49] and D3BJ correction. For molecular dynamics modeling a temperature of 350 K and a SMD continuum model were used to take into account the effect of the solvent (DMF). The time integration step was 1 fs.

Synthesis of product 3

Eosin Y (3 mg, 4.3 μmol), thiol (0.3 mmol), DBU (50 μl, 0.33 mmol) were dissolved in 3ml of DMF. The solution was flushed with argon for 15 minutes. After that, the alkyne (0.15 mmol) was added under argon flow and the cap was closed. The reaction was irradiated by 1.25 W green LEDs for 24 h.

Isolation protocol A: After completion of the reaction 10 ml of petroleum ether was added. The organic layer was washed with 20-% KOH solution in water and brine and dried over MgSO$_4$. The solvent was evaporated under reduced pressure and the residue was purified by column chromatography on silica gel Merck 60 μm (petroleum ether / triethylamine 10:0.01).

ARTICLE

Isolation protocol B: After completion of the reaction 10 ml of DCM was added. The organic layer was washed with 20-% KOH solution in water and brine and dried over MgSO$_4$. The solvent was evaporated under reduced pressure and the residue was purified by column chromatography on silica gel Merck 60 μm (petroleum ether / DCM /triethylamine 10:1:0.01).

Synthesis of product 4

Alkyne (0.15 mmol), thiol (0.45 mmol), Eosin Y (3 mg, 4.3 μmol), DBU (75 μl, 0.48 mmol) and 3 ml of DMF were mixed in a reaction vessel under stirring and placed in a photoreactor equipped with green LEDs (λ$_{max}$ = 533 nm). The reaction was carried out in an open tube for 24h. After completion of the reaction 10 ml of DCM was added. The organic layer was washed with water and brine and dried over MgSO$_4$. The solvent was evaporated under reduced pressure and the residue was purified by column chromatography on silica gel Merck 60 μm (petroleum ether / ethyl acetate, 4:1).

Synthesis of product 5

Alkyne (1 mmol), thiol (1.1 mmol), Eosin Y (6.5 mg, 0.001 mmol), pyridine (25 μl, 0.3 mmol) and 0.5 ml of DMF were mixed in a reaction vessel under stirring and placed in a photoreactor equipped with green LEDs (λ$_{max}$ = 533 nm). The reaction was carried out in an open tube for 6 h. After completion of the reaction 10 ml of DCM was added. The organic layer was washed with water and brine and dried over MgSO$_4$. The solvent was evaporated under reduced pressure and the residue was purified by column chromatography on silica gel Merck 60 μm (petroleum ether).

Synthesis of product 6

Alkyne (1 mmol), thiol (1.5 mmol), ^{t}BuOK (92.5 mg, 0.5 mmol) and 0.5 ml of DMF were mixed in a reaction vessel under stirring. The reaction was carried out in a PTFE screw-capped tube at 70 °C for 24 h. After completion of the reaction 10 ml of DCM was added. The organic layer was washed with water and brine and dried over MgSO$_4$. The solvent was evaporated under reduced pressure and the residue was purified by column chromatography on silica gel Merck 60 μm (petroleum ether).

Product **7hb** was obtained by column chromatography on silica gel Merck 60 μm (petroleum ether / dichloromethane / triethylamine 10:1:0.01) from reaction mixture of **3hb**.

Synthesis of product 4ob'

Thiol (**2b**) (0.3 mmol), Eosin Y (3 mg, 4.3 μmol), K$_2$CO$_3$ (40 mg) and 3 ml DMF were placed into a PTFE screw-capped tube under stirring. The solution was flushed under argon for 10 minutes. After that acetylene **1o** (0.15 mmol) was added in the argon flow and cap was closed hermetic. The reaction vessel was put into the photoreactor equipped with green LEDs (W = 30 W, λ$_{max}$ = 533 nm) and stirring was conducted for 24 h. After completion of the reaction 10 ml of DCM was added. The organic layer was washed with water and brine and dried over MgSO$_4$. The solvent layer was evaporated under reduced

pressure and the residue was purified from column chromatography on silica gel Merck 60 μm (petroleum ether / ethyl acetate, 4:1).

Synthesis of product 4pb

Thiol (**2b**) (0.3 mmol), Eosin Y (3 mg, 4.3 μmol), K$_2$CO$_3$ (40 mg) and 3 ml DMF were placed into a PTFE screw-capped tube under stirring. The solution was flushed with argon for 10 minutes. After that *o*-(*o*-bromphenyl)phenylacetylene (**1p**) (0.15 mmol) was added under argon flow and the cap was closed hermetically. The reaction was placed in a photoreactor equipped with green LEDs (W = 30 W, λ$_{max}$ = 533 nm) and allowed to proceed for 24 h under stirring. After completion of the reaction 10 ml of DCM was added. The organic layer was washed with water and brine and dried over MgSO$_4$. The solvent was evaporated under reduced pressure and the residue was purified by column chromatography on silica gel Merck 60 μm (petroleum ether / ethyl acetate, 5:1).

Synthesis of product 8na

Thiol (**2a**) (0.45 mmol), Eosin Y (6.5 mg, 0.001 mmol), K$_2$CO$_3$ (69 mg) and in 3ml of DMF were placed into a PTFE screw-capped tube under stirring. The solution was flushed with argon for 10 minutes. After that, *o*-bromphenylacetylene (**1n**) (0.15mmol) was added under argon flow and the cap was closed hermetically. The reaction was placed in a photoreactor equipped with green LEDs (λ$_{max}$ = 533 nm) and allowed to proceed for 24 h under stirring. After completion of the reaction 10 ml of DCM was added. The organic layer was washed with water and brine and dried over MgSO$_4$. The solvent was evaporated under reduced pressure and the residue was purified by column chromatography on silica gel Merck 60 μm (petroleum ether).

Monitoring of the photocatalytic thiol-yne click reaction by irradiation in the ionization chamber

Alkyne (**1q**) (11.6 mg, 30 μmol), 1,8-diazabicyclo[5.4.0]undec-7-ene (DBU) (10 μl, 66 μmol), 3 mg (4.3 μmol) of eosin Y and 4ml of DMF were mixed in a round-bottom flask, and arylthiol (**2d**) (7 μl, 62 μmol) was added. An aliquot of the reaction mixture was injected into the ESI ion source of the mass spectrometer. After 10 min the green laser (80 mW) was turned on and the reaction monitoring was started after stabilization of the total ion current. The products were detected in negative ion mode as singly charged ions.

Conflicts of interest

There are no conflicts to declare.

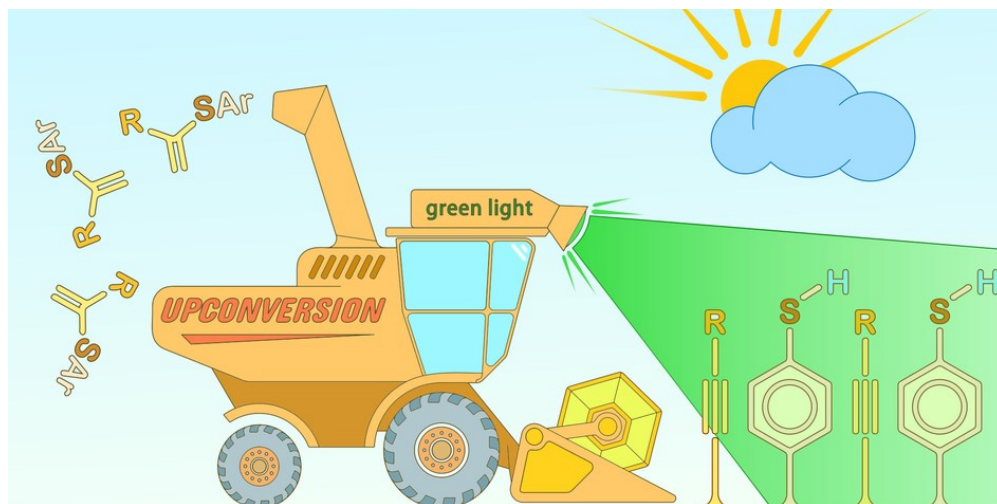## Notes and references

1   P. Chauhan, S. Mahajan and D. Enders, *Chem. Rev.*, 2014, **114**, 8807–8864.

2   I. P. Beletskaya and V. P. Ananikov, *Chem. Rev.*, 2011, **111**, 1596–1636.

Chemical Science Accepted Manuscript

3   A. Ogawa, T. Ikeda, K. Kimura and T. Hirao, *J. Am. Chem. Soc.*, 1999, **121**, 5108–5114.

4   A. Ishii and N. Nakata, in *Hydrofunctionalization*, eds. V. P. Ananikov and M. Tanaka, Springer Berlin Heidelberg, Berlin, Heidelberg, 2013, pp. 21–50.

5   R. Chinchilla and C. Nájera, *Chem. Rev.*, 2014, **114**, 1783–1826.

6   A. Ogawa, in *Hydrofunctionalization*, eds. V. P. Ananikov and M. Tanaka, Springer Berlin Heidelberg, Berlin, Heidelberg, 2013, pp. 325–360.

7   N. V Orlov, *ChemistryOpen*, 2015, **4**, 682–697.

8   R. Castarlenas, A. Di Giuseppe, J. J. Pérez-Torrente and L. A. Oro, *Angew. Chemie Int. Ed.*, 2013, **52**, 211–222.

9   E. O. Pentsak, D. B. Eremin, E. G. Gordeev and V. P. Ananikov, *ACS Catal.*, 2019, 3070–3081.

10   R. H. Crabtree, *Chem. Rev.*, 2012, **112**, 1536–1554.

11   A. S. Kashin and V. P. Ananikov, *J. Org. Chem.*, 2013, **78**, 11117–11125.

12   N. A. Romero and D. A. Nicewicz, *Chem. Rev.*, 2016, **116**, 10075–10166.

13   C. K. Prier, D. A. Rankic and D. W. C. MacMillan, *Chem. Rev.*, 2013, **113**, 5322–5363.

14   J. M. R. Narayanam and C. R. J. Stephenson, *Chem. Soc. Rev.*, 2011, **40**, 102–113.

15   J. Zhu, W. C. Yang, X. D. Wang and L. Wu, *Adv. Synth. Catal.*, 2018, **360**, 386–400.

16   S. S. Zalesskiy, N. S. Shlapakov and V. P. Ananikov, *Chem. Sci.*, 2016, **7**, 6740–6745.

17   S. Kaur, G. Zhao, E. Busch and T. Wang, *Org. Biomol. Chem.*, 2019, **17**, 1955–1961.

18   H. Wang, Q. Lu, C. W. Chiang, Y. Luo, J. Zhou, G. Wang and A. Lei, *Angew. Chemie - Int. Ed.*, 2017, **56**, 595–599.

19   P. G. Theobald and W. H. Okamura, *J. Org. Chem.*, 1990, **55**, 741–750.

20   L. A. Carpino and M. Philbin, *J. Org. Chem.*, 1999, **64**, 4315–4323.

21   M. A. Syroeshkin, F. Kuriakose, E. A. Saverina, V. A. Timofeeva, M. P. Egorov and I. V Alabugin, *Angew. Chemie Int. Ed.*, 2019, **58**, 5532–5550.

22   Q. Elliott, G. dos Passos Gomes, C. J. Evoniuk and I. V Alabugin, *Chem. Sci.*, 2020.

23   P. W. Peterson, N. Shevchenko, B. Breiner, M. Manoharan, F. Lufti, J. Delaune, M. Kingsley, K. Kovnir and I. V Alabugin, *J. Am. Chem. Soc.*, 2016, **138**, 15617–15628.

24   A. Kondoh, K. Takami, H. Yorimitsu and K. Oshima, *J. Org. Chem.*, 2005, **70**, 6468–6473.

25   Y. Zhou, J. Wang, Z. Gu, S. Wang, W. Zhu, J. L. Acenã, V. A. Soloshonok, K. Izawa and H. Liu, *Chem. Rev.*, 2016, **116**, 422–518.

26   M. G. Campbell and T. Ritter, *Chem. Rev.*, 2015, **115**, 612–633.

27   T. Fujiwara and D. O'Hagan, *J. Fluor. Chem.*, 2014, **167**, 16–29.

28   B. Janhsen, C. G. Daniliuc and A. Studer, *Chem. Sci.*, 2017, **8**, 3547–3553.

29   P. Camargo Solórzano, F. Brigante, A. B. Pierini and L. B. Jimenez, *J. Org. Chem.*, 2018, **83**, 7867–7877.

30   R. R. Knowles, H. G. Yayla, H. Wang, K. T. Tarantino and H. S. Orbe, *J. Am. Chem. Soc.*, 2016, 138, 10794–10797.

31   A. S. Kashin, E. S. Degtyareva, D. B. Eremin and V. P. Ananikov, *Nat. Commun.*, 2018, **9**, 1–12.

32   L. P. E. Yunker, R. L. Stoddard and J. S. McIndoe, *J. Mass Spectrom.*, 2014, **49**, 1–8.

33   S. Chen, Q. Wan and A. K. Badu-Tawiah, *Angew. Chemie - Int. Ed.*, 2016, **55**, 9345–9349.

34   Y. Cai, J. Wang, Y. Zhang, Z. Li, D. Hu, N. Zheng and H. Chen, *J. Am. Chem. Soc.*, 2017, **139**, 12259–12266.

35   J. Zelenka and J. Roithová, *ChemBioChem*, 2020, 1–10.

36   J. S. McIndoe and K. L. Vikse, *J. Mass Spectrom.*, 2019, **54**, 466–479.

37   A. Godsk Larsen, A. Hjarbæk Holm, M. Roberson and K. Daasbjerg, *J. Am. Chem. Soc.*, 2001, **123**, 1723–1729.

38   A. D. Boese and J. M. L. Martin, *J. Chem. Phys.*, 2004, **121**, 3405–3416.

39   A. D. McLean and G. S. Chandler, *J. Chem. Phys.*, 1980, **72**, 5639–5648.

40   R. Krishnan, J. S. Binkley, R. Seeger and J. A. Pople, *J. Chem. Phys.*, 1980, **72**, 650–654.

41   T. Clark, J. Chandrasekhar and G. W. Spitznagel, *J. Comput. Chem.*, 1983, **4**, 294–301.

42   X. Gime, J. M. Bofill and J. Gonza, *J. Comput. Chem.*, 2007, **28**, 2111–2121.

43   S. Grimme, J. Antony, S. Ehrlich and H. Krieg, *J. Chem. Phys.*, , DOI:10.1063/1.3382344.

44   A. V Marenich, C. J. Cramer and D. G. Truhlar, *J. Phys. Chem. B*, 2009, **113**, 6378.

45   F. MJ., 2009.

46   S. S. Iyengar, H. B. Schlegel, J. M. Millam, G. A. Voth, G. E. Scuseria and M. J. Frisch, *J. Chem. Phys.*, 2001, **115**, 10291–10302.

47   H. B. Schlegel, J. M. Millam, S. S. Iyengar, G. A. Voth, A. D. Daniels, G. E. Scuseria and M. J. Frisch, *J. Chem. Phys.*, 2001, **114**, 9758–9763.

48   H. B. Schlegel, S. S. Iyengar, X. Li, J. M. Millam, G. A. Voth, G. E. Scuseria and M. J. Frisch, *J. Chem. Phys.*, 2002, **117**, 8694–8704.

49   F. Weigend and R. Ahlrichs, *Phys. Chem. Chem. Phys.*, 2005, **7**, 3297–3305.

79x39mm (300 x 300 DPI)